Petrology and spatial correlation of Black Belly tuff cone basalts, Tanzania

N. Halász and T. M. Tóth
Department of Mineralogy, Geochemistry and Petrology; University of Szeged, 6722 Szeged,
Egyetem street 2-6, Hungary
e-mail: halasznoemi94@gmail.com; 0000-0002-4996-4033; mtoth@geo.u-szeged.hu; 0000-0003-1012-1095
Corresponding Author: halasznoemi94@gmail.com

Abstract

Most of the tuff cones in the North Tanzanian region have not been studied in depth. Therefore, the range of known rock types is limited, and the relationships between these cones are unknown. Our study focused on the Black Belly tuff cone located close to Oldoinyo Lengai. Petrographically, the studied Black Belly samples are alkaline basalts with microcrystalline groundmass and phenocrysts. The groundmass consists of plagioclase, clinopyroxene, Ti-magnetite, apatite, and the phenocrysts are predominantly clinopyroxene, altered (to calcite and serpentinite) olivine, and carbonate minerals. While Oldoinyo Lengai and Black Belly rocks are not similar or directly related, the mineralogy and mineral chemistry of the studied Black Belly samples are similar to those representing the Crater Highlands' volcanoes. Based on their compositions, the Black Belly clinopyroxenes define one end-member, and Oldoinyo Lengai clinopyroxenes represent the other end-member, while the Crater Highlands' samples are of a transitional composition. The compositions of the other minerals (olivine, feldspar, and magnetite) confirm this theory. According to mineral chemical data, the Black Belly samples crystallised in several steps under high pressures (5.6 to 6.6 kbar) and temperatures (750 to 900°C) from an alkali basaltic melt. Considering the new chemical and thermobarometry mineral data presented here and the structural evolution of the region, Black Belly cannot be petrologically part of Oldoinyo Lengai. Instead, it defines an end-member of a series, with Oldoinyo Lengai representing the other extreme and the Crater Highlands volcanoes in a transitional position.

Introduction

The East African Rift System is a 3 700 km long system from Ethiopia to Mozambique through Kenya and Tanzania, containing several volcanoes with diverse rock types and heterogeneous compositions. Our study area lies along the Gregory Rift (Eastern Branch of the East African Rift System), where the volcanism started 30 million years ago at the northern part, in Ethiopia; and 6 million years ago at the study area, in North Tanzania (Dawson, 2008).

One of the volcanic areas of North-Tanzania is the Crater Highlands, built by various volcanoes mostly with basaltic compositions, such as Ngorongoro, Lemagurut, Oldeani, Olmoti, Embagai, and Ogol (Mollel, 2007). In general, these volcanoes produce basaltic rocks with clinopyroxene, feldspar, and oxide phases, with, in some cases, olivine, mica, and apatite. Both alkali and plagioclase feldspars are present as primary magmatic minerals (Mollel, 2007). Beside basalts, trachyte, foidite, phonolite and rhyolite also occurs at these volcanoes (Mana et al., 2012), however we focused on basalts in this study.

In addition to common alkali-rich basalts, unique rock types such as carbonatites also occur in the North Tanzanian Volcanic Province. A unique and widely known carbonatite volcano is Oldoinyo Lengai, the Earth's only active natrocarbonatite producer. The volcano's body is built mainly of nephelinite and phonolite, containing clinopyroxene (aegirine-augite), nepheline, garnet, apatite, combeite, wollastonite, and diverse oxide phases (Dawson, 2008) and is highly peralkaline.

Oldoinyo Lengai eruptions, besides its well-known natrocarbonatite and peralkaline extrusive rocks, have also brought unusual alkaline plutonic rocks, such as ijolites and olivine melilitites, to the surface as xenoliths (Keller et al., 2006; Dawson, 2008). These rocks are characterised by a mineral assemblage of olivine, clinopyroxene (aegirine-augite), nepheline, melilite, wollastonite, mica, and garnet. While most constituents are primary magmatic phases, the origin of the olivine is controversial (in all rock types), as it may be either a primary magmatic phase (Keller et al., 2006; Giuliani, 2018; Baudouin and Parat, 2020; Halász et al., 2023) or a mantle-sourced derived xenocryst (Dawson and Smith, 1988, 1992a; Dawson et al., 1995; Sekisova et al., 2015).

Alongside the basaltic and carbonatite-producing volcanoes, many parasitic cones occur across the entire volcanic province. Oldoinyo Lengai's parasitic cones commonly produced olivine melilitites (Keller et al., 2006). It has been suggested that all melilititic tuff cones close to Oldoinyo Lengai are probably related to the central volcano (Dawson et al., 1985; Peterson and Kjarsgaard, 1995; Johnson et al., 1997). One such cone is Black Belly, a flat tuff ring located on the northwestern flank of Oldoinyo Lengai (Keller et al., 2006). The current study focuses on this area, where previously examined rocks essentially comprise olivine melilitites (Keller et al., 2006). However, our studied samples from Black Belly are basalts, something which was not described from the area before.

The fact that Black Belly lies on the flank of Oldoinyo Lengai and that they have similar rock types (olivine-melilitites) raise the question about the relation of the two, so we chose to compare our studied samples with Oldoinyo Lengai samples. The newly found basaltic rocks made it important to choose some basaltic volcanoes as a comparison too, so beside Oldoinyo Lengai we also compared the studied Black Belly samples with the Crater Highlands basalts.

Sampling and methods

Dozens of volcanic rock samples were collected from the Black Belly tuff cone field (Longitude: -2.623254, Latitude: 35.904846) by Tibor Guzmics and two representative samples were selected from a suite of mafic rocks.

Petrographic observations were carried out in the Department of Mineralogy, Geochemistry and Petrology, University of Szeged, using Brunel-SP-300-P and Olympus BX 41 optical microscopes. For the mineral chemistry, Energy Dispersive X-Ray Spectroscopy (EDS – with silicon drift detector – SDD) (Quantax75) combined with a microscope (TM4000Plus; Hitachi) was used for the ELTE Faculty of Science Research and Instrument Core Facility with instrument settings of 15 kV accelerating voltage, 833 pA beam current, and 15 seconds counting times. Natural standards were used for the instrument calibration, and complete ZAF corrections were applied. Cathodoluminescence (CL) microscopic observations were performed with a CL instrument (Reliotron VII) mounted on a microscope (BX43; Olympus). The operation parameters were 7 kV and 0.7 mA.

Geological background

Our study area, Black Belly and the other associated areas – Oldoinyo Lengai and Crater Highlands – lie in the North Tanzanian Divergence (Figure 1). This region lies between the Tanzania craton and the Mozambique orogenic fold belt (Dawson, 2008). The Tanzania craton is a composite of Archean metasediments and is composed of greenstone belts (Pinna et al., 1995) intruded by granite plutons (Cahen et al., 1984). The lithologically very complex Mozambique belt formed as part of the Pan-African orogeny (Kennedy, 1964). The volcanism in the North Tanzanian Divergence most probably started in the Late Miocene or Early Pliocene (Dawson, 2008).

Black Belly is a flat tuff ring located on the northwestern flank of Oldoinyo Lengai (Keller et al., 2006). It was considered a bedded pyroclastic sequence containing only olivine melilitites without lava flows (Keller et al., 2006); however, our samples are basalts, a rock type that has not been reported from the Black Belly yet.

Olivine melilitites are common rocks not just at Black Belly but also at Oldoinyo Lengai (Velde and Yoder, 1977; Dawson et al., 1985; Keller and Krafft, 1990; Peterson and Kjarsgaard, 1995; Dawson, 1998; Wiedenmann, 2004; Keller et al., 2006) and in the rift-valley tuff cone field located between Lake Natron and Engaruka area (Dawson and Powell, 1969; Dawson et al., 1985; Mattsson and Tripoli 2011; Mattsson et al., 2013; Peterson and Kjarsgaard, 1995; Johnson et al., 1997). Olivine melilitites are considered as candidates in the area for primary melt compositions and thereby the parental magma to the unique carbonatites of the region (Keller et al., 2006). These rocks are usually identified as moderately fractionated olivine melilititic bombs and blocks in bedded pyroclastics with phenocrysts (i.e., olivine, melilite, nepheline, clinopyroxene, garnet, perovskite, and spinel) and glass (Dawson et al., 1985).

Because of the presence of basalt in Black Belly, the surrounding basaltic volcanoes are also included in our research. Crater Highlands region, besides its nephelinitic volcanism, includes mostly basaltic volcanoes: Ngorongoro, Lemagurut, Oldeani, Olmoti, Embagai, and Ogol (Dawson, 2008). These volcanoes usually produce rocks with the mineral assemblage of olivine, clinopyroxene, feldspar, amphibole, garnet, titanite, rarely sodalite, spinel, and minor mica, apatite, Fe-oxides.

Petrography and mineral chemistry

Both of our Black Belly samples are basalts with similar textures. They consist of clinopyroxene and olivine megacrysts and some carbonate crystals set in a microcrystalline groundmass predominantly composed of clinopyroxene, Ti-magnetite, and feldspar (Figure 2A to F).

Olivine (0.5 to 1.2 mm) has two morphologies:

- euhedral, unzoned, fresh crystals of Fo_{73} (Figure 2A), and
- euhedral, unzoned crystals with compositions of Fo_{74-85}, and containing white and dark alteration rims (Figure 2B).

The white rim is a carbonate zone consisting of calcite with 1.4 to 2.0 wt.% MnO and 4.8 to 8.2 wt.% MgO (Figure 3 and Table 1), while the brown zone contains serpentine minerals (Figure 3

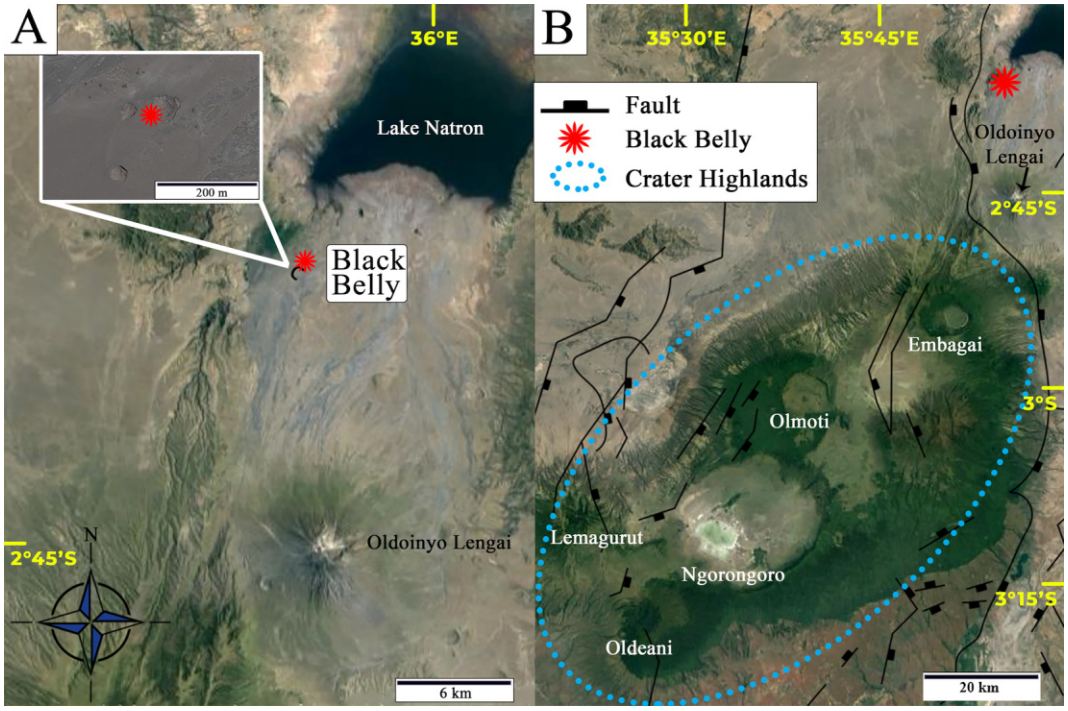

Figure 1. *(**A**) Location of Black Belly area, between Lake Natron and Oldoinyo Lengai volcano. The red star shows the exact place of origin of the studied samples. Inset: picture shows a closer view of the origin of the samples. (**B**) Geological and satellite map of the Black Belly area and Crater Highlands region.*

and Table 1). In some cases, the olivine contains Ti-magnetite as mineral inclusion. Spinel is absent as an inclusion (Figure 2A).

Large (0.5 to 1.5 mm) clinopyroxene phenocrysts are euhedral, brownish-green, and zoned (Figure 2C). Geochemically distinct lighter and darker zones alternate within the grains (Figure 2D and 4A to C). There is evidence of a resorption, suggested by the corroded zone edges (see Figure 4A and B with yellow arrow). These two zones can be distinguished on the element maps (Figure 4C); however, based on the chemical composition (Table 2), both zones are diopside, one of the zones has a slightly more FeO^T and Na_2O rich component (mg# 62 to 75) (Table 2 clinopyroxene 3 and 4). All clinopyroxene contains mineral inclusions of Ti-magnetite, alkali-feldspar (Ab_{72-76}, An_{2-3}, Or_{22-25}; Table 3), carbonate (Figure 2C and Table 1), and melt inclusions (Figure 2E and F). The carbonate minerals are calcite and Mg-rich calcite (Table 1) with similar optical properties.

Some rounded carbonate grains show white-greyish zonation (Figure 5C and D), which is reflected in the chemistry (Table 1). In all the measured grains, the dolomite-rich zone (darker gray in Figure 5), and the calcite-rich zone (lighter grey on the figure) show irregular zonation. This kind of zonation only occurs in the largest (~200 µm) carbonate crystals and does not extend to the carbonate inclusions in the clinopyroxenes.

Raman spectroscopy, scanning electron microscopy (SEM) analysis, and CL were used to study the groundmass minerals, as they could not be identified by optical microscopy (Figure 5A and B). The groundmass clinopyroxenes are diopside (Table 2). The main constituent of the groundmass is a columnar mineral

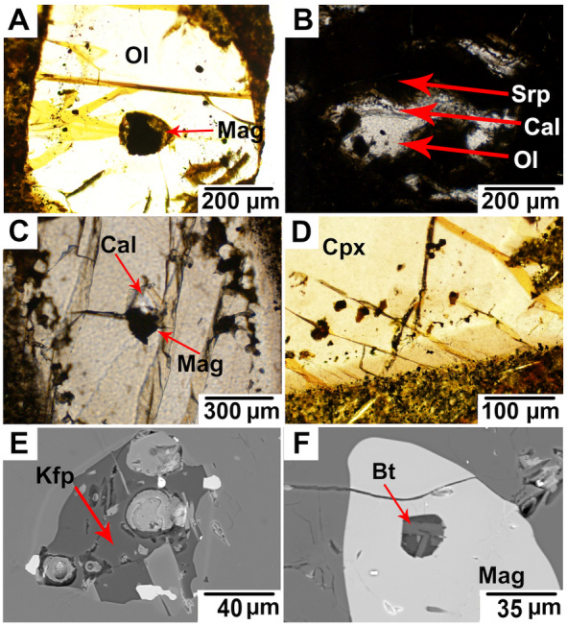

Figure 2. *Representative images of the sample studied [(A) to (D) Plane polarised light (PPL) images, (E) and (F) are backscattered electron (BSE) images]. Euhedral (**A**) and (**B**) xenomorphic, corroded olivine; clinopyroxene with calcite and magnetite inclusions (**C**) zoned clinopyroxene (**D**) crystallised melt inclusion in clinopyroxene, dominated by K-feldspar (**E**) and crystallised melt inclusion in magnetite enclosed in clinopyroxene (**F**). Ol=olivine; Cpx=clinopyroxene; Cal=calcite; Mag=magnetite; Afs=alkali-feldspar; Bt=biotite; Srp=serpentine. Mineral abbreviations are following Whitney, and Evans (2010).*

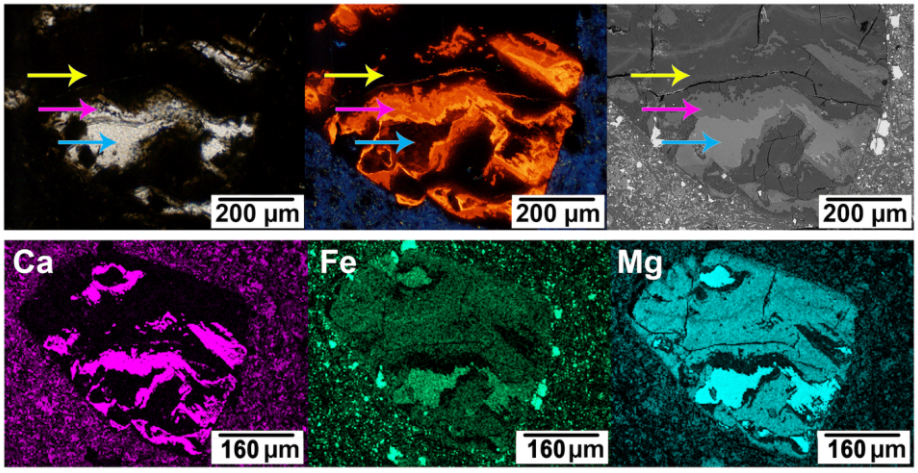

Figure 3. *Textural and compositional features of a xenomorphic olivine grain and its alteration rims. Upper row from left to right: petrographic image in plane polarised light (PPL), Cathodoluminescence (CL) activity image, and backscattered electron (BSE) image. Blue arrow=original olivine; pink arrow=carbonate zone; and yellow arrow=serpentine zone. Lower row from left to right: maps of the same olivine for elements Ca, Fe, Mg.*

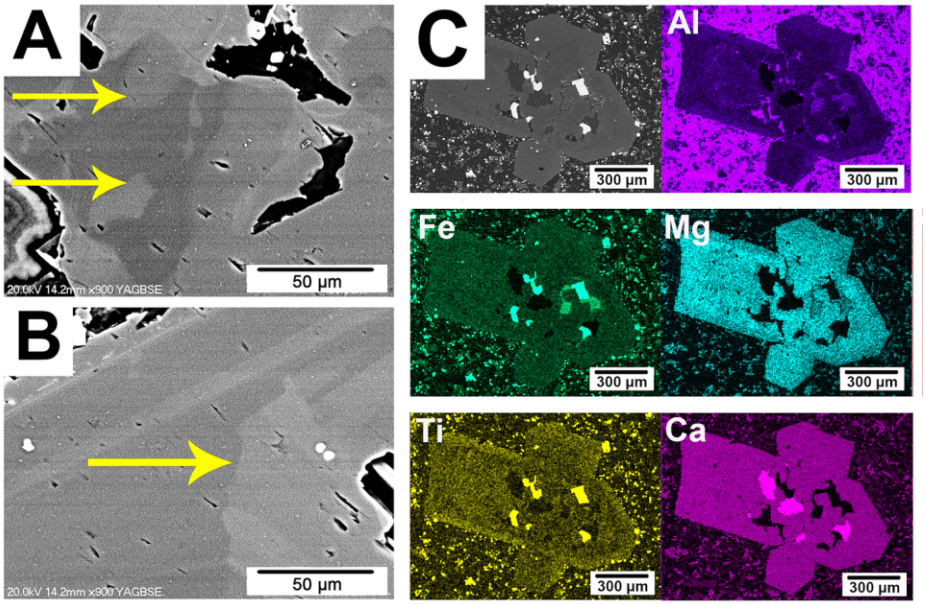

Figure 4. *Backscattered electron (BSE) image of the clinopyroxene zonation, yellow arrow showing the "original" core (**A**) and (**B**). Composition map of a clinopyroxene (**C**) first row from left to right: BSE image of a clinopyroxene, Al content map; on the second and third rows Fe, Mg, Ti and Ca content of the clinopyroxene are shown.*

identified as plagioclase feldspar ($Ab_{42–51}$, $An_{46–54}$, and $Or_{2–3}$) (Table 3). The groundmass also includes tiny, pseudomorphic calcite [replacing probably olivine], Ti-magnetite (Table 3), and apatite.

Cathodoluminescence spectroscopy

The carbonate zone around the olivine phenocrysts shows CL activity (Figure 3) at 625 to 650 nm. These wavelengths lie with the orange colour range, which usually indicates Mn^{2+} between 570 to 640 nm in carbonate minerals (Walker et al., 1989; Machel et al., 1991; Calderon et al., 1996). The olivine has a slight Mn enrichment of 1.4 to 2.0 wt.% at the CL active sites, confirming Mn substitution (Table 1).

The calcite inclusions in the clinopyroxene (Figure 5C and D) are CL active at 615 to 645 nm, also caused by Mn^{2+}. The Mg-rich calcite phenocrysts (MnO ~4, MgO 28 to 30) has a more intensive spectrum and colour than the Mg-poor calcite (MnO 0.004 to 1.7, MgO 1.6 to 2.2), which is explained by its higher Mn content. The Mg-rich calcite zone of the rounded and zoned carbonate crystals (Figure 5C and D) also has a higher Mn content than its calcite zone, with a peak at 600 to 650 nm,

Table 1. Composition of olivine, its alteration rims: calcite and serpentine; and composition of all carbonate minerals.

	Olivine		**Olivine alteration**				**Carbonate**						
			Calcite		**Serpentine**		**In clinopyroxene**			**Phenocryst – calcite**		**Phenocryst – Mg-rich calcite**	
	Euhedral	Anhedral	1	2	1	2	1	2	3	1	2	1	2
SiO_2	37.73	37.34	0.94	1.18	56.15	56.12	1.73	1.59	1.78	1.33	1.27	1.45	5.37
TiO_2	0.18	0.00	0.12	0.04	0.18	0.16	0.24	0.00	0.00	0.04	0.00	0.00	0.15
Al_2O_3	0.27	0.27	0.32	0.30	5.67	4.62	0.57	0.51	0.54	0.71	0.30	0.62	0.72
FeO^T	22.37	23.73	1.66	1.78	12.91	14.84	0.31	0.39	2.21	0.19	0.22	0.01	0.53
Cr_2O_3	0.05	0.00	0.07	0.07	0.00	0.07	0.14	0.00	0.24	0.03	0.00	0.00	0.14
MnO	0.23	0.52	1.37	1.88	0.00	0.00	0.52	0.79	5.80	0.18	0.10	4.18	1.25
MgO	37.70	36.45	8.23	5.67	21.33	20.89	2.52	2.56	30.69	2.17	1.62	28.04	30.57
NiO	0.00	0.28	0.07	0.00	0.10	0.08	0.00	0.00	0.15	0.04	0.00	0.18	0.35
SrO	0.00	0.00	0.00	0.00	0.00	0.00	0.34	0.16	0.16	0.12	0.15	0.43	0.31
CaO	0.47	0.42	84.79	87.62	0.95	0.68	91.19	92.41	56.44	92.24	93.61	62.17	58.50
Na_2O	0.10	0.17	0.27	0.15	1.07	0.98	0.28	0.12	0.14	0.25	0.49	0.56	0.32
K_2O	0.04	0.00	0.13	0.11	0.19	0.25	0.16	0.14	0.21	0.16	0.10	0.14	0.10
SO_3	0.15	0.00	0.33	0.10	0.13	0.00	0.00	0.04	0.00	0.00	0.00	0.01	0.00
Total	99.29	99.18	98.30	98.90	98.68	98.69	98.00	98.71	98.36	97.46	97.86	97.79	98.31
Cations for 4 Oxygen													
Si	0.99	0.99	-	-	-	-	-	-	-	-	-	-	-
Ti	0.00	0.00	-	-	-	-	-	-	-	-	-	-	-
Al	0.01	0.01	-	-	-	-	-	-	-	-	-	-	-
Fe	0.49	0.53	-	-	-	-	-	-	-	-	-	-	-
Cr	0.00	0.00	-	-	-	-	-	-	-	-	-	-	-
Mn	0.01	0.01	-	-	-	-	-	-	-	-	-	-	-
Mg	1.48	1.44	-	-	-	-	-	-	-	-	-	-	-
Ni	0.00	0.01	-	-	-	-	-	-	-	-	-	-	-
Sr	0.00	0.00	-	-	-	-	-	-	-	-	-	-	-
Ca	0.01	0.01	-	-	-	-	-	-	-	-	-	-	-
Na	0.01	0.01	-	-	-	-	-	-	-	-	-	-	-
Sum	3.00	3.01	-	-	-	-	-	-	-	-	-	-	-

Table 2. Composition of clinopyroxene grains. The Fe^{3+} was calculated by the mass ratio of FeO and Fe_2O_3.

	Clinopyroxene							
	Phenocrysts				**Groundmass**			
	1	2	3	4	1	2	3	4
SiO_2	47.03	47.25	47.29	42.88	46.73	44.79	46.87	49.42
TiO_2	2.79	2.96	2.74	4.24	3.01	3.89	2.87	1.97
Al_2O_3	6.48	6.29	6.21	9.22	6.54	7.18	6.49	4.39
FeO^T	7.97	7.64	7.88	11.21	8.47	9.17	8.08	7.31
Cr_2O_3	0.17	0.24	0.13	0.08	0.05	0.14	0.11	0.15
MnO	0.23	0.09	0.00	0.20	0.26	0.04	0.14	0.07
MgO	12.08	12.26	12.62	9.94	11.74	11.97	11.90	13.28
NiO	0.00	0.00	0.04	0.05	0.07	0.00	0.00	0.09
CaO	22.19	22.24	22.23	20.72	22.29	21.51	22.46	22.48
Na_2O	0.59	0.61	0.73	0.95	0.72	0.62	0.58	0.58
Total	99.53	99.58	99.87	99.49	99.88	99.31	99.50	99.74
FeO	6.02	6.17	7.06	10.80	8.24	8.92	7.87	7.13
Fe_2O_3	2.17	1.64	0.91	0.45	0.26	0.27	0.23	0.20
Cations for 6 Oxygen								
Si	1.76	1.77	1.77	1.65	1.76	1.71	1.77	1.85
Ti	0.08	0.08	0.08	0.12	0.09	0.11	0.08	0.06
Al	0.29	0.28	0.27	0.42	0.29	0.32	0.29	0.19
Fe^{II}	0.19	0.19	0.22	0.35	0.26	0.28	0.25	0.22
Fe^{III}	0.06	0.05	0.03	0.01	0.01	0.01	0.01	0.01
Cr	0.01	0.01	0.00	0.00	0.00	0.00	0.00	0.00
Mn	0.01	0.00	0.00	0.01	0.01	0.00	0.00	0.00
Mg	0.68	0.69	0.71	0.57	0.66	0.68	0.67	0.74
Ni	0.00	0.00	0.00	0.00	0.00	0.00	0.00	0.00
Ca	0.89	0.89	0.89	0.85	0.90	0.88	0.91	0.90
Na	0.04	0.04	0.05	0.07	0.05	0.05	0.04	0.04
Sum	4	4	4	4	4	4	4	4
End-members in mol%								
Jadeite	11.79	12.10	11.29	15.72	12.10	12.10	12.26	9.12
Fe-Al Tschermak	14.52	13.35	13.44	19.37	13.68	15.87	13.32	8.81
Aegirine	0.00	0.00	0.00	0.00	0.00	0.00	0.00	0.00
Fe-Fe Tschermak	0.00	0.00	0.00	0.00	0.00	0.00	0.00	0.00
Diopside	62.69	62.99	63.57	48.38	59.25	59.09	59.71	68.82
Hedenbergite	4.66	5.42	3.45	3.91	6.91	1.19	7.41	5.83
Wollastonite	0.00	0.00	0.00	0.00	0.00	0.00	0.00	0.00
Enstatite-ferrosilite	6.33	6.14	8.25	12.63	8.06	11.74	7.30	7.41
Sum	100	100	100	100	100	100	100	100

similar to the previously described carbonate minerals. To clarify the similarities between the different types of carbonates, all carbonate CL activity is summarised in Table 4.

Plagioclase feldspar, the main constituent of the groundmass, shows slight activity as a light-bluish colour (Figure 5D), with two well-defined peaks at 450 to 500 nm and 700 to 750 nm. This is the typical colour for such plagioclase (Table 3). A smaller peak appears at ~550 nm. The bluish light associated with the peak at 450 to 500 nm is common for igneous feldspars (Götze et al., 2000). These properties, typical of feldspars, are caused by an electron-hole recombination structural defect at various hole centers by Ti^{4+} activation or Al^{3+} for Si^{4+} substitution in the crystal lattice (Mariano et al., 1973; Mariano and Ring, 1975; Marfunin, 1979; Götze et al., 2000). The resulting slight CL activity may suggest that the feldspar formed at a lower temperature inside the feldspar stability field (Kastner, 1971; Escobar and Mariano, 1976; Kastner and Silver, 1979).

Table 3. Composition of Ti-magnetite and feldspars (alkali-feldspar and plagioclase). The Fe^{3+} was calculated by the mass ratio of FeO and Fe_2O_3.

	Magnetite						**Feldspar**			
	In clinopyroxene		**In olivine**		**Groundmass**		**Alkali-feldspar in clinopyroxene**		**Plagioclase in groundmass**	
	1	2	1	2	1	2	1	2	1	2
SiO_2	3.80	1.33	1.23	1.10	0.94	1.26	63.42	62.38	55.45	54.05
TiO_2	19.92	18.22	17.47	17.52	21.77	27.39	0.13	0.08	0.38	0.28
Al_2O_3	5.63	4.94	5.57	5.57	4.31	1.38	20.95	18.91	27.41	28.10
FeO^T	66.15	70.61	66.56	65.70	68.02	66.63	0.37	0.36	0.71	0.88
Cr_2O_3	0.36	0.26	4.41	4.59	0.22	0.14	0.04	0.00	0.01	0.00
MnO	0.67	0.73	0.59	0.68	1.00	1.05	0.01	0.00	0.01	0.02
MgO	1.01	3.19	3.65	3.70	2.86	0.72	0.05	0.09	0.00	0.12
NiO	0.00	0.09	0.00	0.26	0.00	0.25	0.02	0.00	0.00	0.24
SrO	0.19	0.00	0.17	0.00	0.21	0.26	0.00	0.00	0.00	0.00
CaO	0.50	0.20	0.06	0.06	0.20	0.34	2.60	1.06	9.44	10.09
Na_2O	0.44	0.27	0.29	0.39	0.31	0.37	7.33	3.17	5.43	4.76
K_2O	0.14	0.05	0.00	0.00	0.00	0.05	3.82	10.07	0.51	0.47
SO_3	0.00	0.00	0.00	0.00	0.03	0.00	0.02	0.05	0.00	0.06
Total	98.81	99.89	100.00	99.57	99.87	99.84	98.76	96.17	99.35	99.07
FeO	46.98	43.51	42.41	42.11	46.77	54.11	-	-	-	-
Fe_2O_3	21.30	30.13	26.85	26.22	23.62	13.91	-	-	-	-
	Cations for 4 Oxygen						**Cations for 8 Oxygen**			
Si	0.00	0.00	0.00	0.00	0.00	0.00	2.87	2.95	2.53	2.48
Ti	0.57	0.49	0.46	0.47	0.59	0.77	-	-	-	-
Al	0.25	0.21	0.23	0.23	0.18	0.06	1.12	1.05	1.47	1.52
Fe^{II}	1.49	1.30	1.25	1.25	1.40	1.70	0.01	0.01	0.03	0.03
Fe^{III}	0.61	0.81	0.71	0.70	0.64	0.39	0.00	0.00	0.00	0.00
Cr	0.01	0.01	0.12	0.13	0.01	0.00	-	-	-	-
Mn	0.02	0.02	0.02	0.02	0.03	0.03	-	-	-	-
Mg	0.06	0.17	0.19	0.20	0.15	0.04	-	-	-	-
Sr	-	-	-	-	-	-	0.00	0.00	0.00	0.00
Ca	-	-	-	-	-	-	0.13	0.05	0.46	0.50
Na	-	-	-	-	-	-	0.64	0.29	0.48	0.42
K	-	-	-	-	-	-	0.22	0.61	0.03	0.03
Sum	3.00	3.00	3.00	3.00	3.00	3.00	5.00	4.97	4.99	4.98

Table 4. Summary for the Cathodolumninescence (CL) active carbonate minerals based on Energy Dispersive X-Ray Spectroscopy (EDS).

	In clinopyroxene				**In olivine**		**Phenocrysts**			
	Mg-rich calcite		**Calcite**		**Calcite**		**Dolo-calcite**		**Calcite**	
CL wave length (nm)	615 to 645				625 to 650		600–650			
Composition in w%	Min	Max	Min	Max	Min	Max	Min	Max	Min	Max
CaO	56.44	56.78	87.16	94.16	83.28	87.62	57.11	62.17	92.24	93.61
MgO	30.69	31.03	0.49	3.05	4.75	8.23	28.04	35.74	1.58	2.17
MnO	4.20	5.80	0.00	2.52	1.35	1.98	1.00	4.18	0.10	0.20
FeO	2.21	2.24	0.11	0.93	1.66	2.12	0.01	1.24	0.07	0.22

Discussion

Mineral comparison and correlation between Black Belly, Oldoinyo Lengai and Crater Highlands

The similarity between Black Belly rocks and Oldoinyo Lengai olivine melilitites could suggest a possible relationship between the two and imply that Black Belly is a parasitic cone to Oldoinyo Lengai. To explore whether the Black Belly samples are genetically related to other eruptive products of Oldoinyo Lengai, we first compared the studied phenocrysts with similar phenocrysts from the plutonic and volcanic rocks of Oldoinyo Lengai and its cones. However, the fact that Black Belly is located on the flank of Oldoinyo Lengai and so erupted through Oldoinyo Lengai's rocks could also explain the similarity.

As we found basalts beside the well-known olivine-melilitites of Black Belly, we also extended the comparison to the surrounding volcanoes of the Crater Highlands.

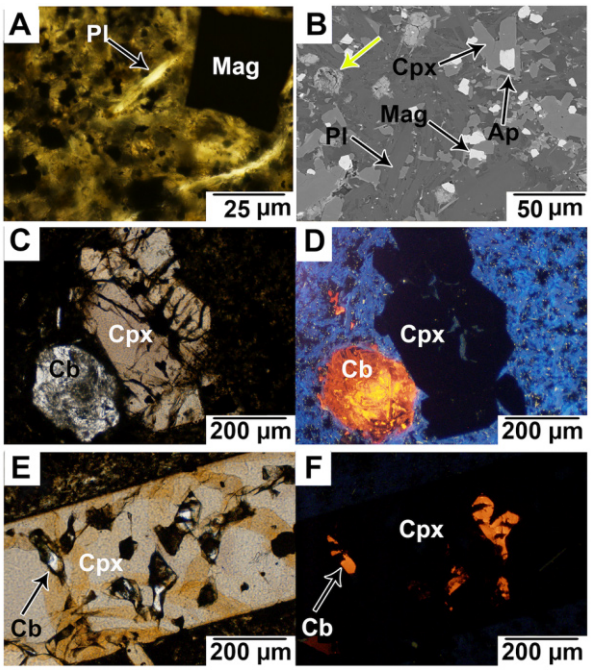

Figure 5. *Groundmass minerals of the studied samples: Ti-magnetite and plagioclase (**A**) and other constituents – plagioclase, magnetite, apatite, clinopyroxene, and olivine pseudomorph, indicated by yellow arrow – (**B**) Petrographic plane polarised light (PPL) and Cathodoluminescence (CL) images of the phases: Carbonate crystals (**C**) and (**D**); calcite inclusions in clinopyroxene (**E**) and (**F**). Mineral abbreviations are following Whitney, and Evans (2010).*

Mineral comparisons

Clinopyroxene

In the studied samples, clinopyroxene occurs as a phenocryst and groundmass mineral with a diopsidic composition and slight growth zonation. Oldoinyo Lengai plutonic rocks (i.e., ijolite, pyroxenite, jacupirangite, and olivine-mica ijolite) usually contain clinopyroxenes in which diopside and aegirine-augite zones shows irregular zonation, while the volcanic rocks (i.e., phonolite and nephelinite) mostly contain aegirine-augite. This zonation is a common phenomenon in most Oldoinyo Lengai rock types (plutonic, parasitic, and volcanic), and it is thought to be the result of magma mixing (Dawson and Smith, 1992; Dawson et al., 1995; Dawson et al., 2008; Carmody, 2012; Sekisova et al., 2015; Halász et al., 2023) before or during the crystallisation of clinopyroxenes. It is important to note that the clinopyroxenes in our samples are not compositionally similar to previously analysed Oldoinyo Lengai clinopyroxenes (diopside, aegirine-augitic clinopyroxenes from both plutonic, and volcanic rocks) (Figure 6). Instead, they are similar to the diopside-hedenbergites from the Crater Highlands volcanoes, including Ogol, Embagai, Lemagurut, and Oldeani (Mollel, 2007; Mollel et al., 2008; Mollel et al., 2011; Greenwood, 2014). Among all Crater Highlands volcanoes, Olmoti is the only one with clinopyroxenes slightly enriched in the aegirine-augitic component; their enrichment pattern is different from Oldoinyo

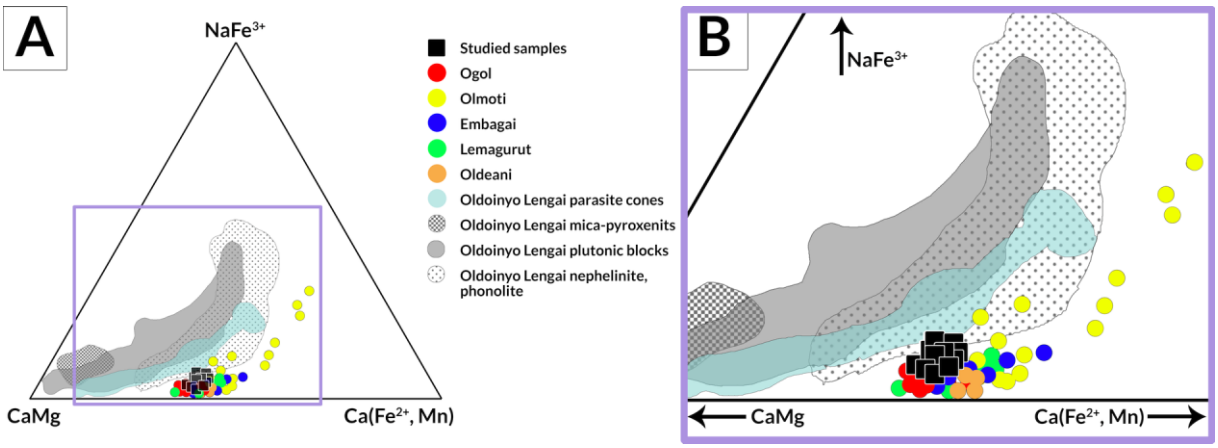

Figure 6. *Comparison of clinopyroxene compositions of Oldoinyo Lengai and Crater Highlands rocks (**A**) and an inset (**B**). All the black squares are stands for Black Belly samples; circles for the Crater Highlands volcanoes, whereas the Oldoinyo Lengai compositions are given as fields (Mollel, 2007; Mollel et al., 2008; Mollel et al., 2011; Greenwood, 2014) similar to our studied samples).*

Lengai aegirine-augitic clinopyroxenes as it s accmponied by a higher hedenbergite component (see yellow circles on Figure 6). All the other volcanoes show a diopside-hedenbergite composition (Figure 6).

Clinopyroxenes of Black Belly are more similar to Crater Highlands' clinopyroxenes, but also not far from Oldoinyo Lengai clinopyroxenes (Figure 6 and Table 2). To better understand any possible relationships, the clinopyroxenes of the region were further examined, and their chemistries were compared. We chose to use Al_2O_3–TiO_2, Na_2O+CaO–TiO_2, SiO_2–MgO, Na_2O–Al_2O_3, Na_2O–TiO_2, and CaO–TiO_2 diagrams for the comparisons (Figure 7A to G).

The Black Belly clinopyroxene phenocrysts are the most Al-rich end-member, while Oldoinyo Lengai clinopyroxenes are the least Al-rich; Black Belly groundmass crystals are intermediate to these compositions and plot closer to the typical Crater Highlands pyroxenes (Figure 7A). The exceptionally high Al_2O_3 content (phenocrysts 3.1 to 10.8 wt.% and groundmass 3.0 to 7.2 wt.%) of the Black Belly clinopyroxenes allows us to use the Al^{IV}–Al^{VI}+Fe^{3+} diagram (Figure 7B) to explore the

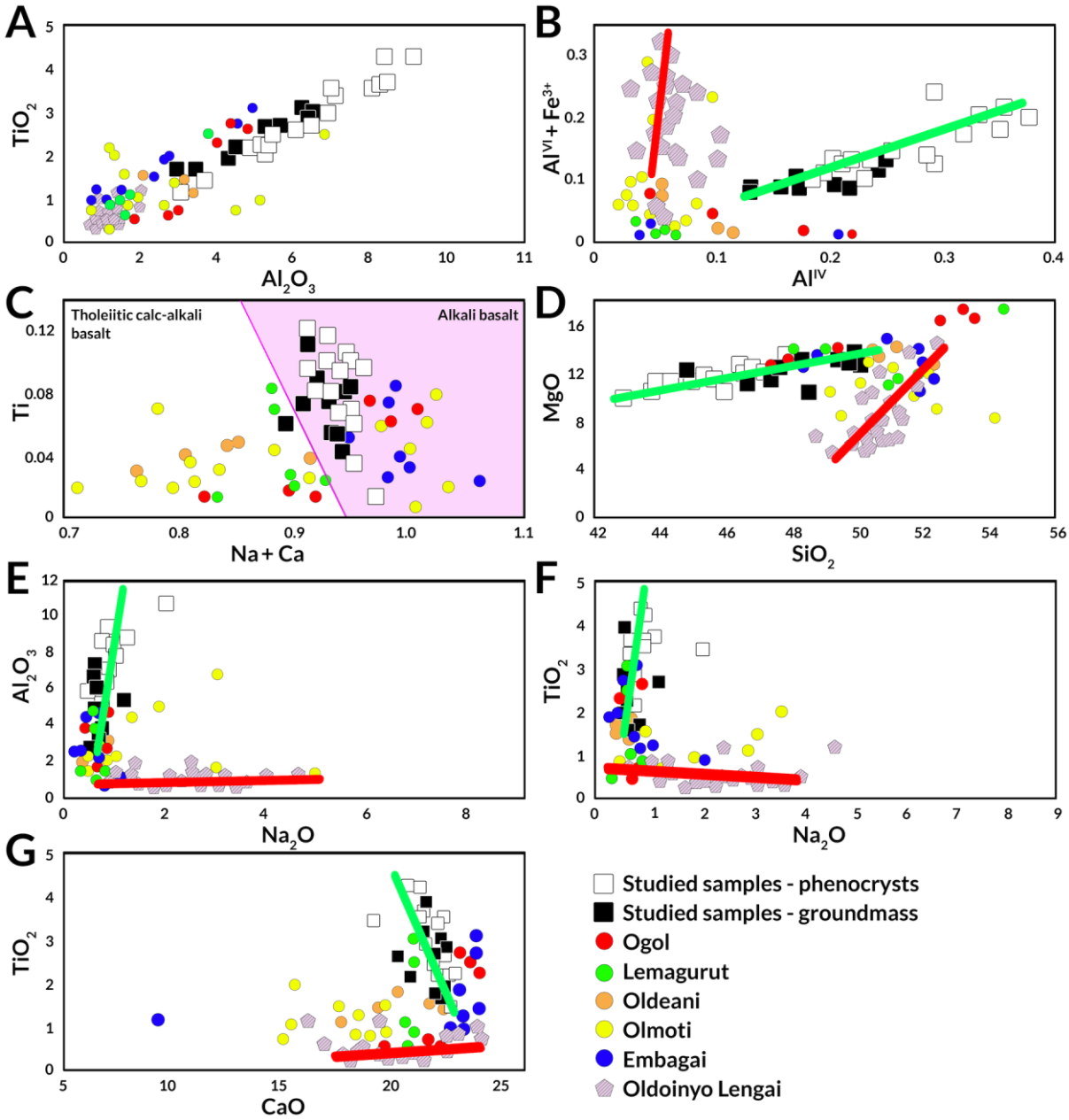

Figure 7. *Diagrams for clinopyroxenes based on these pairs: Al_2O_3 – TiO_2 (**A**), Al^{IV} – Al^{VI}+Fe^{3+} (**B**), Na_2O + CaO – TiO_2 (**C**), SiO_2 – MgO (**D**), Na_2O – Al_2O_3 (**E**), Na_2O – TiO_2 (**F**), CaO – TiO_2 (**G**). Data of the diagrams is from this study, Dawson and Smith 1992; Dawson et al., 1995; Klaudius and Keller 2006; Mollel, 2007; Mollel et al., 2008; Mollel et al., 2011; Greenwood, 2014; Sekisova et al., 2015; Halász et al., 2023. The red line shows the Oldoinyo Lengai trend; the green line shows the Black Belly trend.*

thermobarometric environment of crystal growth. Al in the tetrahedral position is significantly higher for the Black Belly clinopyroxenes compared to the Oldoinyo Lengai and Crater Highlands clinopyroxenes. The presence of Al instead of Si in the tetrahedron indicates Tschermak substitution ($Al^{IV}Al^{VI}Si_{-1}{}^{IV}Mg_{-1}{}^{VI}$), which is temperature and pressure sensitive (Al^{IV} is temperature while Al^{VI} is pressure sensitive; Newton et al., 1977). We thus suggest that Black Belly clinopyroxenes crystallised at higher P and T compared to Crater Highlands and Oldoinyo Lengai clinopyroxenes.

Olivine

The two textural subtypes of olivine (euhedral and anhedral forsterite) overlap on the Ca-Fo diagram (Figure 8).

The compositions representing Black Belly, Oldoinyo Lengai, and the Crater Highlands cover a wide range and each volcano plots separately on Fo-Ca and Fo-Mn diagrams; most likely reflecting compositional differences between the melts from which they crystallised (Dawson and Smith, 1992; Dawson et al., 1995; Sekisova et al., 2015; Halász et al., 2023; Mollel, 2007; Mollel et al., 2008; Mollel et al., 2011; Greenwood, 2014) (Figure 8).

Feldspar

There are two types of feldspars in the studied samples: K-bearing alkali feldspar (anorthoclase) occurs as inclusions in the clinopyroxene, and plagioclase feldspar (andesine, labradorite) can be found in the groundmass. Feldspar is not a common constituent in Oldoinyo Lengai eruptives: primary feldspar is rare in tuff cone rocks (Keller et al., 2006), and it usually occurs in parasitic cone lavas as K-feldspar. In contrast, plagioclase feldspar is a common constituent in the Crater Highlands rocks, and alkali-feldspar also occurs as phenocrysts and in the groundmass (Mollel, 2007; Mollel et al., 2008; Mollel et al., 2011; Greenwood, 2014). The composition of Crater Highlands' feldspars ranges from sanidine to labradorite (Figure 9). The widely accepted origin of feldspars of the region is primary magmatic origin; however, an alternative source for feldspars in the region is suggested. If feldspar and K-rich zeolite minerals (e.g., phillipsite) appear together, it could indicate the significant role of fenitisation (McHenry, 2010; Greenwood, 2014), although the absence of zeolite minerals in the studied samples excludes a late metasomatic origin for the feldspars. Compared with the Crater Highlands feldspars, our studied feldspars are similar in composition to Olmoti, Oldeani, and Lemagurut feldspars, including both groundmass plagioclase and alkali-feldspar inclusions (Figure 9). Our feldspars cover a narrower compositional range (Figure 9), as all the alkali-feldspar grains are anorthoclase, and all the plagioclase feldspar is andesine-labradorite.

Magnetite

Black Belly magnetite can be divided into two groups: the magnetite occurring as inclusions in clinopyroxene has a lower TiO_2 content and greater FeO^T content than the groundmass magnetite. The magnetite grains from Black Belly differ from the Oldoinyo Lengai magnetite grains; however, they are similar to the Crater Highlands magnetite compositions (Figure 10). A difference is also evident in the MnO and MgO content:

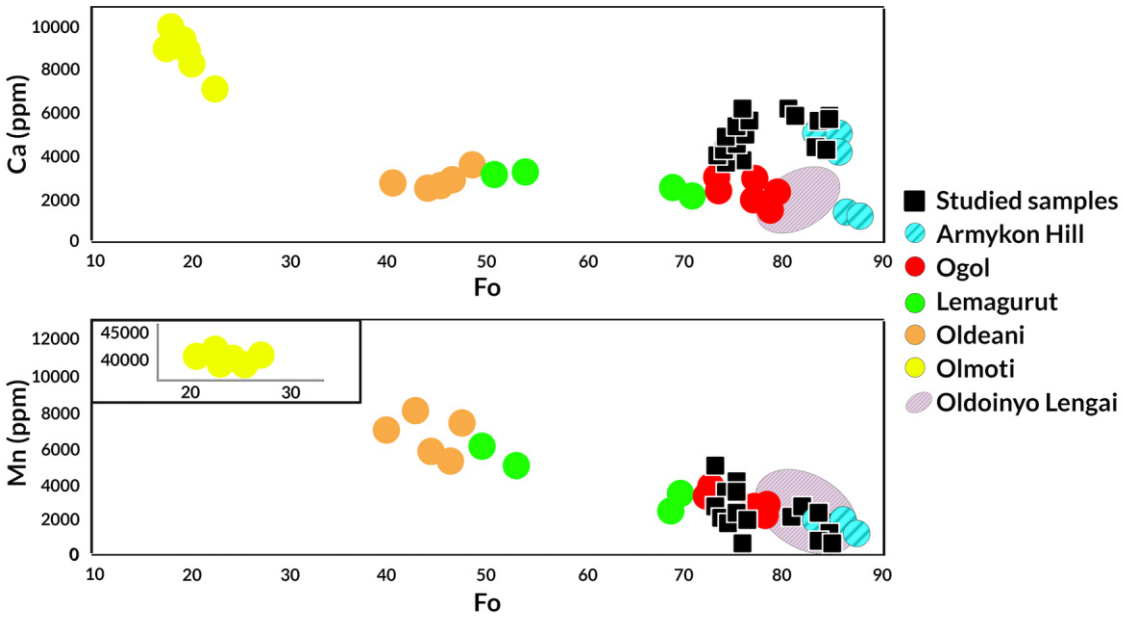

Figure 8. *Olivine compositions of Black Belly, Oldoinyo Lengai and Crater Highlands on Fo-Ca and Fo-Mn diagrams. Based on the accuracy of the Energy Dispersive X-Ray spectroscopy (EDS) method, possibly there is a slight difference between real and measured data.*

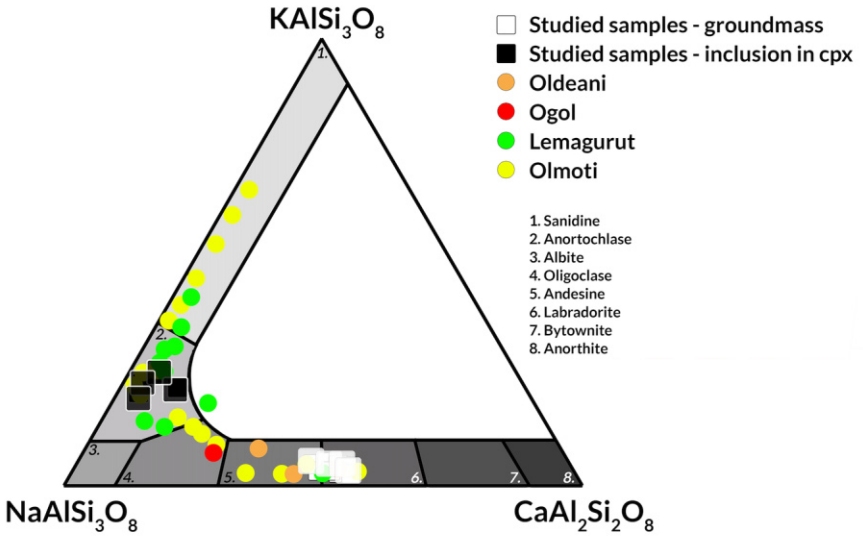

Figure 9. *Feldspars of the studied samples and Crater Highlands rocks.*

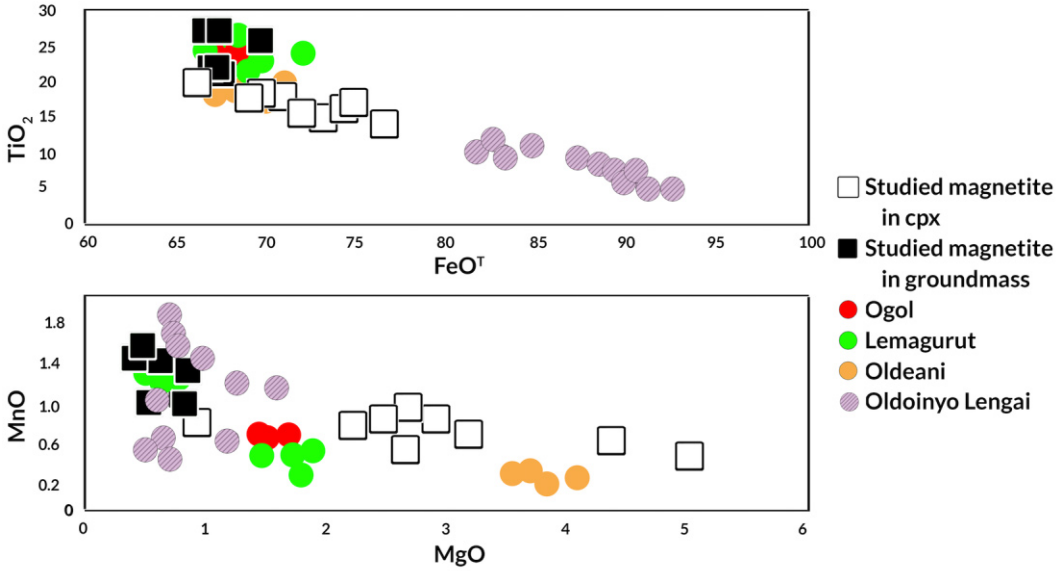

Figure 10. *FeO^T–TiO_2 and MgO–MnO diagrams of magnetites, from this study, Dawson and Smith 1992; Dawson et al., 1995; Mollel 2007; Sekisova et al., 2015; Halász et al., 2023.*

the inclusion magnetite is richer in MgO but poorer in MnO than the groundmass magnetite.

The magnetite grains help us to understand the geodynamical properties of the Black Belly samples. Based on the Mn/Mg ratio (Figure 10), the exact minimum crystallisation temperature of the magnetite grains can be determined by the method of Evans et al. (2016). Magnetite inclusions in clinopyroxene phenocrysts crystallised at >850°C and at ~750°C for the groundmass magnetite. The Mg-content (atomic $Mg/[Mg+Fe^{2+}]$) supports the same temperatures (Evans et al., 2016).

Crystallisation history and geodynamic consequences

Crystallisation of the main constituents: Phenocrysts and groundmass

Based on mineral chemistry and appearance, the Black Belly clinopyroxene phenocrysts represent an early high-P and -T crystallisation stage. Textural evidence for the corrosion of the clinopyroxene edges (Figure 4A and B) indicates that the clinopyroxene phenocrysts likely formed in several stages, with repeated mixing of two slightly different melts (Figure 4A and B).

Alkali-feldspar (anorthoclase) is exclusively present as crystallised melt inclusions in the clinopyroxene phenocrysts.

The presence of K-rich minerals (mica and alkali feldspar) in the crystallised melt inclusions of the clinopyroxene and alkali-feldspar inclusions suggests a K-rich primary magma for the phenocrysts.

Olivine phenocrysts in the studied samples and from the region (Figure 8) have lower mg# (74 to 85) and higher Ca (4 000 to 6 200 ppm) than those derived from lithospheric mantle sources (mg# ≥90 and Ca <1 000 ppm) (Li et al., 2011). The origin of northern Tanzania olivines is controversial. The widely accepted model for Oldoinyo Lengai olivines is a mantle origin (Dawson and Smith, 1988, 1992a; Dawson et al., 1995; Sekisova et al., 2015). However, it has been suggested that olivine is an early magmatic liquidus phase (Keller et al., 2006; Giuliani, 2018; Baudouin and Parat, 2020; Halász et al., 2023). The higher Fo content and lower Ca content of mantle olivine (Li et al., 2011) compared to the studied olivines suggest that the olivine was formed during primary magmatic crystallisation at an early stage. Olivine was probably one of the earliest phases to crystallise from an alkali basaltic melt. The presence of magnetite inclusions in the olivine and clinopyroxene phenocrysts indicates an approximate minimum crystallisation temperature of >850°C (Evans et al., 2016). There is a possibility that this temperature does not reflect tha original crystallisation but a later re-equilibration.

Following the formation of phenocrysts, the groundmass crystallised during a cooling period at ~750°C (based on magnetite data).

The role of carbonate minerals in petrogenesis

All carbonate minerals in the studied samples have similar chemistries (Table 1), appearances, and CL activities (Table 4), suggesting a similar origin. Primary magmatic carbonates are rare in the area, following Greenwood (2014), an abundance of carbonates can be related to a saline crater lake, fumarole activity, and the alteration of carbonatite ash derived from the nearby volcanoes Oldoinyo Lengai and Kerimasi. Saline crater lakes are present in the area; Lake Embagai is located within the eastern part of the Embagai caldera at 2209 m (Dawson, 2008; Greenwood, 2014). Given that Black Belly and Embagai are located close to each other, and Kerimasi is close to Oldoinyo Lengai, the origin of their carbonate grains may be similar. Accordingly, we suggest the same source for the carbonate minerals as Greenwood (2014): the carbonates originated from carbonatite ash or formed due to postmagmatic activities, and some are secondary minerals due to the reactions of olivine.

Geodynamic consequences

The studied Black Belly samples are different from previously described Black Belly rocks (Keller et al., 2006) as the basalts are predominantly composed of clinopyroxene, feldspar, olivine, and magnetite, while melilite is entirely absent. This new result extends not only our petrographic knowledge of Black Belly but also our understanding of its geodynamic origin and context. Until now, as an exclusively olivine-melilitite bearing tuff cone, Black Belly has been genetically connected to Oldoinyo Lengai and regarded as a possible parasitic cone. However, knowing that basalts also occur at Black Belly, which do not occur in the Oldoinyo Lengai system, this relationship is improbable. We suggest that the similarity between Black Belly olivine-melilitites and Oldoinyo Lengai olivine melilitites is because of the fact that Black Belly is located on the flank of Oldoinyo Lengai and so erupted through it and so the olivine melilitites were brought up as xenoliths.

We found two separate trends based on clinopyroxene study: the Black Belly and Oldoinyo Lengai trends (Figure 7). This further supports the hypothesis that the Black Belly magmatism is not related to Oldoinyo Lengai.

Black Belly basalts and Crater Highlands basalts are similar in terms of their mineral assemblages, textures, and mineral chemistries, raising the possibility of a genetic relationship between the two areas. However, our detailed clinopyroxene study (Figure 7) showed slight differences between the compositions of the Crater Highlands and Black Belly clinopyroxenes. Crater Highlands clinopyroxenes do not fit the Black Belly trend; they usually plot between the Black Belly and Oldoinyo Lengai trends. Thus, they typify a transitional composition between the two end-members.

While we have geophysical data from Black Belly and Oldoinyo Lengai area, we do not have it from Crater Highlands area. Based on earthquake studies (Reiss et al., 2021) a magma body is located beneath Oldoinyo Lengai at 10 to 15 km; while there is another one at 17 to 20 km depth in the area, where Black Belly is found (Reiss et al., 2021).

Our study showed that Black Belly is not the parasite cone of Oldoinyo Lengai and the similarity between the olivine-melilitites of both volcano could be because of Black Belly's olivine-melilitites are xenoliths as Black Belly lies on the flank of Oldoinyo Lengai and therefore erupts through it. The presence of basaltic rocks at Black Belly suggests that Black Belly is a separate magmatic system, not part of Oldoinyo Lengai. Crater Highlands, Oldoinyo Lengai, and the Black Belly area are all parts of the North Tanzanian Volcanic Province and lie along the same fault branch (Figure 1). Although they are related to each other and parts of the same volcanic system, they are not directly linked to each other.

Conclusion

The Black Belly samples were formed in several stages from an alkali basaltic melt. The mineralogy of the studied samples (e.g., the absence of melilite and the composition of the clinopyroxene, feldspar, and magnetite) does not correlate with previously reported Black Belly rocks. We find no close similarity between the studied Black Belly rocks and those that comprise the nearby volcanic territories of Oldoinyo Lengai and the Crater Highlands. This observation suggests that Black Belly is not part of magmatic systems that support either Oldoinyo Lengai or the Crater Highlands.

Based on our results, Black Belly should be considered an individual volcanic area and should not be seen as a solely olivine-melilitite site. Black Belly is a bedded pyroclastic sequence containing olivine melilitites and basalts, so it is a heterogeneous volcanic area.

Acknowledgments

This research was supported by the ÚNKP-21-2 and ÚNKP-22-3 New National Excellence Programs of the Ministry for Innovation and Technology from the source of the National Research, Development and Innovation Fund. The manuscript has been edited for English language and spelling by Enago, an editing brand of Crimson Interactive Inc. All the studied samples are belonging to Tibor Guzmics and we appreciate the fact that he made them available to us for this research and also special thanks to his help on the research. We are grateful to Tanya Furman and Marlina Elburg, for the detailed suggestions given for the improvement of the manuscript. Thank you for Felix Schubert for his help with the CL experiments.

References

Baudouin, C. and Parat, F., 2020. Phlogopite-Olivine Nephelinites Erupted During Early Stage Rifting, North Tanzanian Divergence. Frontiers in Earth Sciences, 8:277 https://doi.org/10.3389/feart.2020.00277

Bowden, P., 1985. The geochemistry and mineralization of alkaline ring complexes in Africa (a review). Journal of African Earth Sciences, 3, 17-39.

Calderon, T., Townsend, P.D., Beneitez, P., Garcia–Guinea, J., Millan, A., Rendell, H.M., Tookey, A., Urbina, M. and Wood, R.A., 1996. Crystal field effects on the thermoluminescence of manganese in carbonate lattices. Radiation Measurements, 26, 719-731.

Carmody, L., 2012. Geochemical characteristics of carbonatite-related volcanism and subvolcanic metasomatism at Oldoinyo Lengai, Tanzania. Unpublished PhD thesis University College London. 338pp

Dawson, J.B., 1992. Neogene tectonics and volcanicity in the North Tanzania sector of the Gregory rift valley: contrasts with the Kenya sector. Tectonophysics, 204, 81-92.

Dawson, J.B., 1998. Peralkaline nephelinite-natrocarbonatite relationships at Oldoinyo Lengai, Tanzania. Journal of Petrology, 39, 2077-2095.

Dawson, J.B., 2008. The Gregory Rift Valley and Neogene-Recent Volcanoes in Northern Tanzania. Geological Society, London Memoirs. 106pp

Dawson, J.B. and Powell, D.G., 1969. The Natron-Engaruka explosion crater area, Northern Tanzania. Bulletin Volcanologique, 33, 761-817.

Dawson, J.B., Smith, J.V. and Jones, A.P., 1985. A comparative study of bulk rock and mineral chemistry of olivine melilitites and associated rocks from East and South Africa. Neues Jahrbuchfür Mineralogie, Abhandlungen, 152, 143-175.

Dawson, J.B. and Smith, J.V., 1992. Olivine-mica pyroxenite xenoliths from northern Tanzania: metasomatic products of upper-mantle peridotite. Journal of Volcanology and Geothermal Research 50, 131-142.

Dawson, J.B. and Steele, I.M., 1995. Petrology and mineral chemistry of plutonic igneous xenoliths from the carbonatite volcano, Oldoinyo Lengai, Tanzania. Journal of Petrology, 33, 797-826.

Donaldson, C.H., Dawson, J.B., Kanaris-Sotiriou, R., Batchelor, R.A. and Walsh, J.N., 1987. The silicate lavas of Oldoinyo Lengai, Tanzania. Neues Jahrbuch für Mineralogie. Abhandlungen, 156, 247-279.

Escobar, R. and Mariano, A.N., 1976. On the origin of Colombian emeralds. 2nd biannual meeting of the Mineralogical Society of America, Tucson, Abstract

Evans, B.V., Hildreth, W., Bachmann, O. and Scaillet, B., 2016. In defense of magnetite-ilmenite thermometry in the Bishop Tuff and its implication for gradients in silicic magma reservoirs. American Mineralogist, 101, 469-482.

Götze, J., Krbetschek, M.R., Habermann, D. and Wolf, D., 2000. High-resolution cathodoluminescence studies of feldspar minerals. In: M. Pagel, V. Barbin, P. Blanc and D. Ohnenstetter (Editors), Cathodoluminescence in Geosciences. Springer-Verlag Berlin Heidelberg GmbH, 245-270

Greenwood, S.M., 2014. Mineralogy and Geochemistry of Pleistocene Volcanics at Embagai Caldera and Natron Basin, Tanzania: Potential Constraints on the Stratigraphy of Olduvai Gorge. Unpublished PhD thesis, University of Wisconsin-Milwaukee. 497pp

Giuliani, A., 2018. Insights into kimberlite petrogenesis and mantle metasomatism from a review of the compositional zoning of olivine in kimberlites worldwide. Lithos, 312-342.

Halász, N., Berkesi, M., M. Tóth, T., Mitchell, R.H., Milke, R. and Guzmics, T., 2023. Reconstruction of magma chamber processes preserved in olivine-phlogopite micro-ijolites from the Oldoinyo Lengai, Tanzania. Journal of African Earth Sciences, 197, 1-16

Hay, R., 1976. Geology of the Olduvai Gorge: a Study of Sedimentation in a Semi-arid Basin. University of California Press, Berkeley. 220pp

Hay, R., 1987. Geology of Laetoli area. In: M.D. Leakey and J.M. Harris (Editors), A Pliocene site in northern Tanzania. Clarendon Press, Oxford, 23-47.

Johnson, L.H., Jones, A.P., Church, A.A. and Taylor, W.R., 1997. Ultramafic xenoliths and megacrysts from a melilitite tuff cone, Deeti, northern Tanzania. Journal of African Earth Sciences, 25, 29-42.

Kastner, M., 1971. Authigenic feldspars in carbonate rocks. American Mineralogist, 56, 1403-1442.

Kastner, M. and Siever, R.S., 1979. Low temperature feldspars in sedimentary rocks. American Journal of Science, 279, 435-479.

Keller, J., Zaitsev, A.N. and Wiedenmann, D., 2006. Primary magmas at Oldoinyo Lengai: The role of olivine melilitites. Lithos, 91, 150-172.

Keller, J. and Krafft, M., 1990. Effusive natrocarbonatite activity of Oldoinyo Lengai, June 1988. Bulletin of Volcanology, 52, 629-645.

Klaudius, J. and Keller, J. 2006. Peralkaline silicate lavas at Oldoinyo Lengai, Tanzania. Lithos, 91, 173-190.

Le Gall, B., Nonnotte, P., Rolet, J., Benoit, M., Guillou, H. and Mousseau-Nonnotte, M., 2008. Rift propagation at craton margin. Distribution of faulting and volcanism in the North Tanzanian Divergence (East Africa) during Neogene times. Tectonophysics, 448, 1-19.

Li, C., Thakurta, J. and Ripley, E.M., 2011. Low-Ca contents and kink-banded textures are not unique to mantle olivine: evidence from the Duke Island Complex, Alaska. Mineralogy and Petrology, 104, 147-153.

Machel, H.G., Mason, R.A., Mariano, A.N. and Mucci, A., 1991. Causes and emission of luminescence in calcite and dolomite. In: C.E. Baker and O.C. Kopp (Editors), Luminescence microscopy and spectroscopy: qualitative and quantitative applications. Society for Sedimentary Geology, 9-25.

Mana, S., Furman, T., Turrin, B.D., Feigenson, M.D. and Swisher, C.C., 2015. Magmatic activity across the east African north Tanzanian divergence zone. Journal of the Geological Society, 172, 368-389.

Manega, P.C., 1993. Geochronology, Geochemistry and Isotopic Study of the Plio-Pleistocene hominid sites and the Ngorongoro Volcanic Highlands in Northern Tanzania. Unpublished PhD thesis, University of Colorado. 764pp

Marfunin, A.S., Bershov, L.V., Meilman, M.L. and Michoulier, J., 1967. Paramagnetic resonance of Fe^{3+} in some feldspars. Schweizerische Mineralogische und Petrographische Mitteilungen, 47, 13-20.

Mariano, A.N., Ito, J. and Ring, P.J., 1973. Cathodoluminescence of plagioclase feldspars. Geological Society America, 5, 726.

Mariano, A.N. and Ring, P.J., 1975. Europium-activated cathodoluminescence in minerals. Geochimica et Cosmochimica Acta, 39, 649-660.

Mattsson, H.B. and Tripoli, B.A., 2011. Depositional characteristics and volcanic landforms in the Lake Natron-Engaruka monogenetic field, northern Tanzania. Journal of Volcanology and Geothermal Research, 203, 23-34.

Mattsson, H.B., Nandedkar, R.H. and Ulmer, P., 2013. Petrogenesis of the melilititic and nephelinitic rock suites in the Lake Natron–Engaruka monogenetic volcanic field, northern Tanzania. Lithos, 179, 175-192.

McHenry, L.J., Mollel, G.F. and Swisher III, C.C., 2008. Compositional and textural correlations between Olduvai Gorge Bed I tephra and volcanic sources in the Ngorongoro Volcanic Highlands, Tanzania. Quaternary International, 178, 306-319.

McHenry, L.J., 2010. Element distribution between coexisting authigenic mineral phases in argillic and zeolitic altered tephra Olduvai Gorge, Tanzania. Clays and Clay Minerals, 58, 627-643.

Mollel, G.F., 2002. Petrology and geochemistry of the southeastern Ngorongoro Volcanic Highland (NVH); and contribution to "sourcing" of stone tools at Olduvai Gorge, Tanzania. Unpublished Masters Thesis, Rutgers University, New Brunswick, New Jersey. 183pp

Mollel, G.F., 2007. Petrochemistry and geochronology of Ngorongoro Volcanic Highland Complex (NVHC) and its relationship to Laetoli and Olduvai Gorge, Tanzania. Unpublished PhD thesis, Rutgers University, New Brunswick, New Jersey. 254pp

Mollel, G.F., Swisher, III, C.C., Feigenson, M.D. and Carr, M.J., 2011. Petrology, geochemistry, and age of Satiman, Lemagurut and Oldeani: sources of the volcanic deposits of the Laetoli area. In: T. Harrison (Editor), Paleontology and Geology of Laetoli: Human Evolution in Context 1. Springer Dordrecht, 99-119

Mollel, G.F., Swisher III, C.C., Feigenson, M.D. and Carr, M.J., 2008. Geochemical evolution of Ngorongoro Caldera, Tanzania: implications for crust-magma interaction. Earth and Planetary Sciences Letters, 271, 337-347.

Newton, R.C., Charlu, T.V. and Kleppa, O.J., 1977. Thermochemistry of high pressure garnets and clinopyroxenes in the system CaO–MgO–Al_2O_3–SiO_2. Geochimica Cosmochimica Acta, 41, 369- 377.

Peterson, T.D. and Kjarsgaard, B.A., 1995. What are the parental magmas at Oldoinyo Lengai? In: K. Bell and J. Keller (Editors), Carbonatite Volcanism: Oldoinyo Lengai and the Petrogenesis of Natrocarbonatites. Springer Verlag, Berlin, 148-162.

Reiss, M.C., Muirhead, J.D., Laizer, A.S., Link, F., Kazimoto, E.O., Ebinger, C.J. and Rümpker, G. 2021. The Impact of Complex Volcanic Plumbing on the Nature of Seismicity in the Developing Magmatic Natron Rift, Tanzania. Frontiers of Earth Sciences. 8:609805. doi: https://doi.org/10.3389/feart.2020.609805

Robins, B., 1984. Petrography and petrogenesis of nephelinized metagabbros from Finnmark, Northern Norway. Contributions to Mineralogy and Petrology, 86, 170-177.

Rubie, D.C. and Gunter, W.D. 1983. The Role of Speciation in Alkaline Igneous Fluids during Fenite Metasomatism. Contributions to Mineralogy and Petrology, 82, 165-175.

Sekisova, V.S., Sharygin, V.V., Zaitsev, A.N. and Strekopytov, S., 2015. Liquid immiscibility during crystallisation of forsterite-phlogopite ijolites at Oldoinyo Lengai Volcano, Tanzania: Study of melt inclusions. Russian Geology and Geophysics, 56, 1717-1737.

Velde, D. and Yoder Jr., H.S., 1977. Melilite and melilite-bearing igneous rocks. Year B. Carnegie Institution of Washington, 76, 478-485.

Walker, G., Abumere, O.E. and Kamaluddin, B., 1989. Luminescence spectroscopy of Mn^{2+} centres in rock-forming carbonates. Mineralogical Magazine, 53, 201-211.

Wiedenmann, D., 2004. Vulkanologische Stellung und petrologische Interpretation der Biotit Pyroxen-Olivin-Tuffe am Oldoinyo Lengai, Tansania. Unpublished Master thesis, Freiburg. 89pp

Whitney, D. and Evans, B.W., 2010. Abbreviations for names of rock-forming minerals. American Mineralogist, 95, 185-187.

Zharikov, V.A., Pertsev, N.N., Rusinov, V.L., Callegari, E. and Fettes, D.J., 2007. Metasomatism and metasomatic rocks. Recommendations by the IUGS Subcommission on Metamorphic Rocks: Web version 01.02.07. 17pp

Editorial handling: M.A. Elburg.